Article

Current Biology

Encoding of Odor Fear Memories in the Mouse Olfactory Cortex

Highlights

- Fos tagging marks sparse ensembles of piriform neurons active during odor learning
- Chemogenetic silencing of Fos-tagged neurons impairs odor fear memory retrieval
- Reactivation of Fos-tagged neurons mimics odor-evoked memory recall
- Piriform cortex is an essential substrate for olfactory learning and memory

Authors

Claire Meissner-Bernard, Yulia Dembitskaya, Laurent Venance, Alexander Fleischmann

Correspondence

alexander_fleischmann@brown.edu

In Brief

Meissner-Bernard et al. use cFos-based genetic tagging to visualize and manipulate the activity of odor memory trace cells in the mouse piriform cortex. They report that olfactory fear conditioning marks sparse ensembles of piriform neurons, which are critical for odor fear memory recall.

Meissner-Bernard et al., 2019, Current Biology *29*, 367–380
February 4, 2019
https://doi.org/10.1016/j.cub.2018.12.003

CellPress

Current Biology
Article

Encoding of Odor Fear Memories in the Mouse Olfactory Cortex

Claire Meissner-Bernard,[1,3] Yulia Dembitskaya,[1] Laurent Venance,[1] and Alexander Fleischmann[1,2,4,*]
[1]Center for Interdisciplinary Research in Biology (CIRB), Collège de France, and CNRS UMR 7241 and INSERM U1050, Paris, France
[2]Department of Neuroscience and the Robert J. and Nancy D. Carney Institute for Brain Science, Brown University, Providence, RI 02912, USA
[3]Present address: Friedrich Miescher Institute for Biomedical Research, 4058 Basel, Switzerland
[4]Lead Contact
*Correspondence: alexander_fleischmann@brown.edu
https://doi.org/10.1016/j.cub.2018.12.003

SUMMARY

Odor memories are exceptionally robust and essential for animal survival. The olfactory (piriform) cortex has long been hypothesized to encode odor memories, yet the cellular substrates for olfactory learning and memory remain unknown. Here, using intersectional, *cFos*-based genetic manipulations ("Fos tagging"), we show that olfactory fear conditioning activates sparse and distributed ensembles of neurons in the mouse piriform cortex. We demonstrate that chemogenetic silencing of these Fos-tagged piriform ensembles selectively interferes with odor fear memory retrieval but does not compromise basic odor detection and discrimination. Furthermore, chemogenetic reactivation of piriform neurons that were Fos tagged during olfactory fear conditioning causes a decrease in exploratory behavior, mimicking odor-evoked fear memory recall. Together, our experiments identify specific ensembles of piriform neurons as critical components of an olfactory fear memory trace.

INTRODUCTION

Odor perception and behavioral responses to odors strongly depend on experience, and learned odor-context associations often last for the lifetime of an animal [1]. The cellular and neural circuit mechanisms underlying olfactory learning and memory, however, remain poorly understood. Recent studies on episodic and contextual learning in the hippocampus and cortex have suggested that memories are encoded in distributed ensembles of neurons, often referred to as a "memory trace" or "engram" [2, 3]. These engram cells are thought to store information about the environmental context and associated emotions of past experiences, and their activity is necessary and sufficient for memory recall [4–6].

Here, we investigate the organization of odor memories in the olfactory (piriform) cortex of mice. The piriform cortex (PCx), a trilaminar paleocortical structure, is the largest cortical area receiving direct afferent inputs from the olfactory bulb, which, in turn, receives topographically organized inputs from olfactory sensory neurons in the nose. Individual piriform neurons respond to combinatorial inputs from multiple olfactory bulb projection neurons [7, 8], suggesting that odor objects are constructed in the PCx from the molecular features of odorants extracted in the periphery [9]. The PCx has long been hypothesized to support auto-associative network functions that can retrieve previously learned information from partial or degraded sensory inputs [9, 10]. Piriform pyramidal cells form a large recurrent network, which is reciprocally connected with high-order associative areas including the prefrontal, entorhinal, and perirhinal cortex and the amygdala [11, 12]. Storage of information is made possible by NMDA-dependent, associative plasticity of connections [13–15]. Furthermore, changes in piriform network activity [16–18] and stabilization of odor representations [19] have been observed after associative olfactory learning. Finally, excitotoxic lesions of the posterior PCx in rats perturb odor fear memories [20], and optogenetic stimulation of artificial piriform ensembles is sufficient to drive learned behaviors [21]. Taken together, these studies have led to the hypothesis that piriform neural ensembles encode olfactory memory traces.

We have adapted an intersectional genetic strategy to target components of odor fear memories in the PCx. We combined *cFos*-tTA transgenic mice [22], in which the tTA transcription factor is expressed under the promoter of the immediate-early gene *cFos*, with virally targeted expression of tTA-responsive fluorescent reporters and regulators of neural activity [23–25]. This approach allows us to selectively and persistently "Fos tag" piriform neurons that were activated during olfactory fear conditioning. We then tested the behavioral consequences of manipulating such Fos-tagged piriform ensembles during memory recall. We find that chemogenetic silencing of Fos-tagged piriform ensembles interferes with a learned odor escape behavior. In contrast, silencing piriform neurons Fos tagged during presentation of a neutral odor only partially attenuates odor fear memory recall, suggesting that memory impairments are largely specific to the piriform ensemble that is Fos tagged during learning. Finally, artificial reactivation of Fos-tagged piriform neurons elicits behavioral changes consistent with memory recall. Together, our results suggest that piriform neural ensembles encode an essential component of olfactory fear memories.

RESULTS

Behavioral Expression of Odor Fear Memory Depends on the Retrieval Context

We used classical conditioning to train mice to associate an odor with foot shock (the reinforced conditioned stimulus; CS^+) [21].

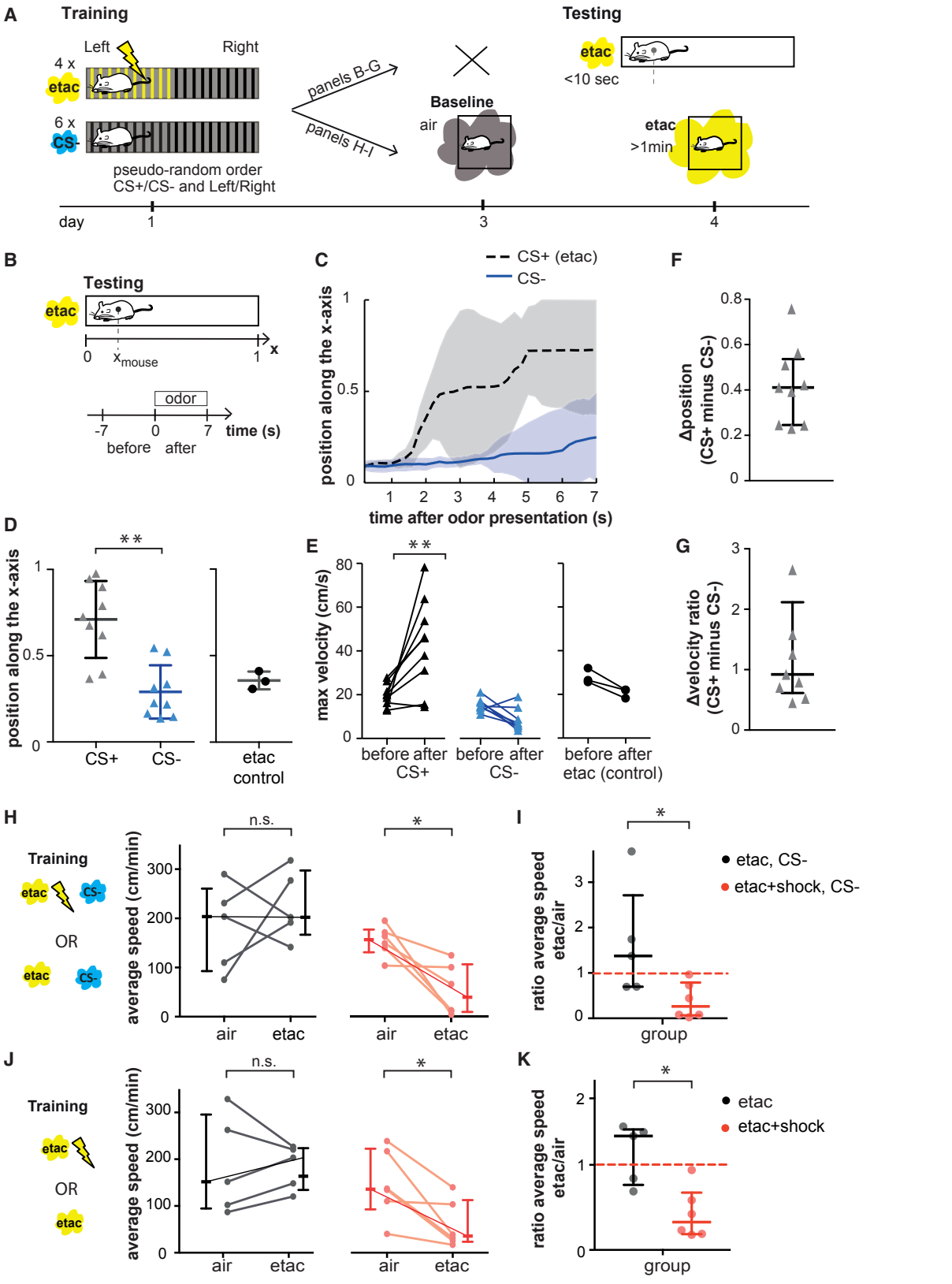

(legend on next page)

Training occurred in a rectangular box with odor ports at each extremity. Brief odor stimuli (7 s) were presented on randomly alternating sides when mice were close to the odor port. The CS^+ (ethyl acetate) was paired with a foot shock, applied to the side of the box where the odor was delivered. Mice escaped from the foot shock by running toward the opposite side of the box (see STAR Methods and Figure 1A). Two control odors, whose presentation was not paired with foot shock (non-reinforced stimuli; CS^-), were used to entrain specific as opposed to generalized fear responses to odors [17]. Memory retrieval of *cFos*-tTA transgenic mice (n = 9) was first tested by presenting the odors alone in a similar context as during conditioning: the same stimulus duration and a testing box with the same dimensions as the training box but with a different texture and color (see STAR Methods). We combined two parameters to quantify the learned escape behavior: the position of the mouse in the box and the increase in its maximum velocity after odor presentation (Figure 1B). These parameters were chosen because they described well the behavioral response of mice to the odor-foot shock pairing during training (Figure S1). The median position of the mice in the box at the end of stimulus delivery was 0.71 (with 0 defined as the site of odor presentation and 1 as the opposite end of the box), and mice exhibited a 1.8-fold increase of their maximum velocity. Importantly, the escape behavior was specific to the CS^+, as none of the mice ran away from the CS^- (Figures 1C–1E). We then subtracted the position after CS^- presentation from the position after CS^+ presentation, and subtracted the CS^- maximum velocity ratio (after/before presentation) from the CS^+ one. A value of 0 would indicate a generalized learned response to odors (escape from the CS^+ and the CS^-) or no learning. Here, the values were significantly different from 0 (Wilcoxon signed-rank test [WSRT], W = 45, p = 0.0039 for both the position and velocity ratio; Figures 1F and 1G).

During both training and testing, odors were presented at the extremities of the box, and the training and testing boxes had the same shape and dimensions. Therefore, contextual features (visual and/or tactile) could be an important determinant for successful memory retrieval. To assess the context dependence of the memory, we tested memory retrieval in a different context. We monitored mouse behavior in an open field during ambient and prolonged odor exposure, where the odor does not originate from a spatially defined odor source as during training (Figure 1A). We fear conditioned mice to ethyl acetate as described above (n = 6). Mice exposed to ethyl acetate without foot shock served as a control (n = 5). Diffusion of ethyl acetate above the open field caused a significant decrease in exploratory behavior of fear-conditioned mice compared to control mice (Mann-Whitney test [MWT], U = 0, p = 0.0043; Figures 1H and 1I). Baseline exploratory behavior measured 1 day earlier did not differ between fear-conditioned and control mice (MWT, U = 11, p = 0.5368). These data suggest that re-exposure of mice to the CS^+ induced memory recall, expressed as a decrease in exploratory behavior in the open-field test. Similar results were obtained when mice were trained only with a CS^+ and no CS^- (MWT, U = 2, p = 0.0173 for ratio; Figures 1J and 1K). The differences in behavioral responses we observe in the two contexts (escape versus decreased exploratory behavior) likely reflect the adaptivity of fear [26].

Figure 1. Behavioral Expression of Odor Fear Memory Depends on the Retrieval Context

(A) During fear conditioning, mice are trained to associate ethyl acetate (CS^+) with foot shock. The CS^+ is presented at one end of a rectangular training box, and the corresponding half-side of the box is electrified. Training includes the presentation of two other odors that are not paired with foot shock (CS^-, eugenol and beta-citronellol). The CS^+ is presented 4 times (2 times on each side) and each CS^- is presented 3 times, for 7 s each. The order and side of odor presentations are pseudo-randomized (see Figure S1). Memory retrieval is tested 3 days later, either in a rectangular testing box or in an open field, with very short or prolonged odor exposure, respectively. In the open field, baseline exploratory activity in the absence of odor (air) is measured 1 day earlier.

(B–J) Wild-type mice are used for testing odor-evoked fear memory recall in the open field, and *cFos*-tTA mice injected with AAV-GCaMP are used for testing in the rectangular testing box.

(B–G) Memory retrieval in a box having the same shape and dimensions as the training box.

(B) In the rectangular testing box, the CS^+ is presented 4 times (2 times on each side), and each CS^- is presented once on each side, for 7 s each. The testing session is video recorded and the position of the mouse's centroid in the box along the x axis is extracted. The length of the box is normalized to 1. Because the odor is presented randomly on the left or right side of the testing box, 0 is defined as the extremity where the odor is presented. For velocity measurements, a 7 s time window is defined both before and after stimulus onset.

(C) Averaged position of mice as a function of time after CS^+ (black dashed line) and CS^- (blue line) presentation.

(D and E) 3 additional mice (ethyl acetate [etac] control) did not receive foot shock after ethyl acetate presentation.

(D) Position in the testing box 7 s after CS^+, CS^-, or etac presentation. Mice are farther away from the odor port after CS^+ presentation than after CS^- presentation (n = 9, W = 45, p = 0039).

(E) Maximum velocity during the 7 s before and 7 s after CS^+ (left), CS^- (middle), or etac (right) presentation. After CS^+ presentation, the maximum velocity significantly increases (n = 9, W = 43, p = 0.0078).

(F) Position 7 s after CS^- presentation subtracted from the position 7 s after CS^+ presentation.

(G) Maximum velocity ratio after/before CS^- subtracted from the maximum velocity ratio after/before CS^+ presentation.

(H–K) Memory retrieval in an open field. Ethyl acetate is presented above the open field from minute 15 to 18 (testing). To measure baseline exploratory activity, air is diffused above the open field the day before (baseline). Ethyl acetate exposure led to a decrease in exploratory behavior in mice previously fear conditioned to ethyl acetate (n = 6, in red). Previous exposure to ethyl acetate without foot shock does not alter exploratory behavior upon re-exposure to ethyl acetate (n = 5, in black).

(H and I) Training includes the presentation of two other odors that are not paired with foot shock (CS^-).

(H) Average speed in cm/min. As a measure for exploratory activity, the distance traveled is computed from minute 15 to 18 (corresponding to odor exposure during testing).

(I) Average speed ratio testing/baseline.

(J and K) Experimental design: same as in (H) and (I), except that training does not include the presentation of CS^-.

(J) Average speed in cm/min.

(K) Average speed ratio testing/baseline.

Dots and triangles represent individual mice; averaged data are shown as median and interquartile range. *p < 0.05, **p < 0.01; n.s., not significant.

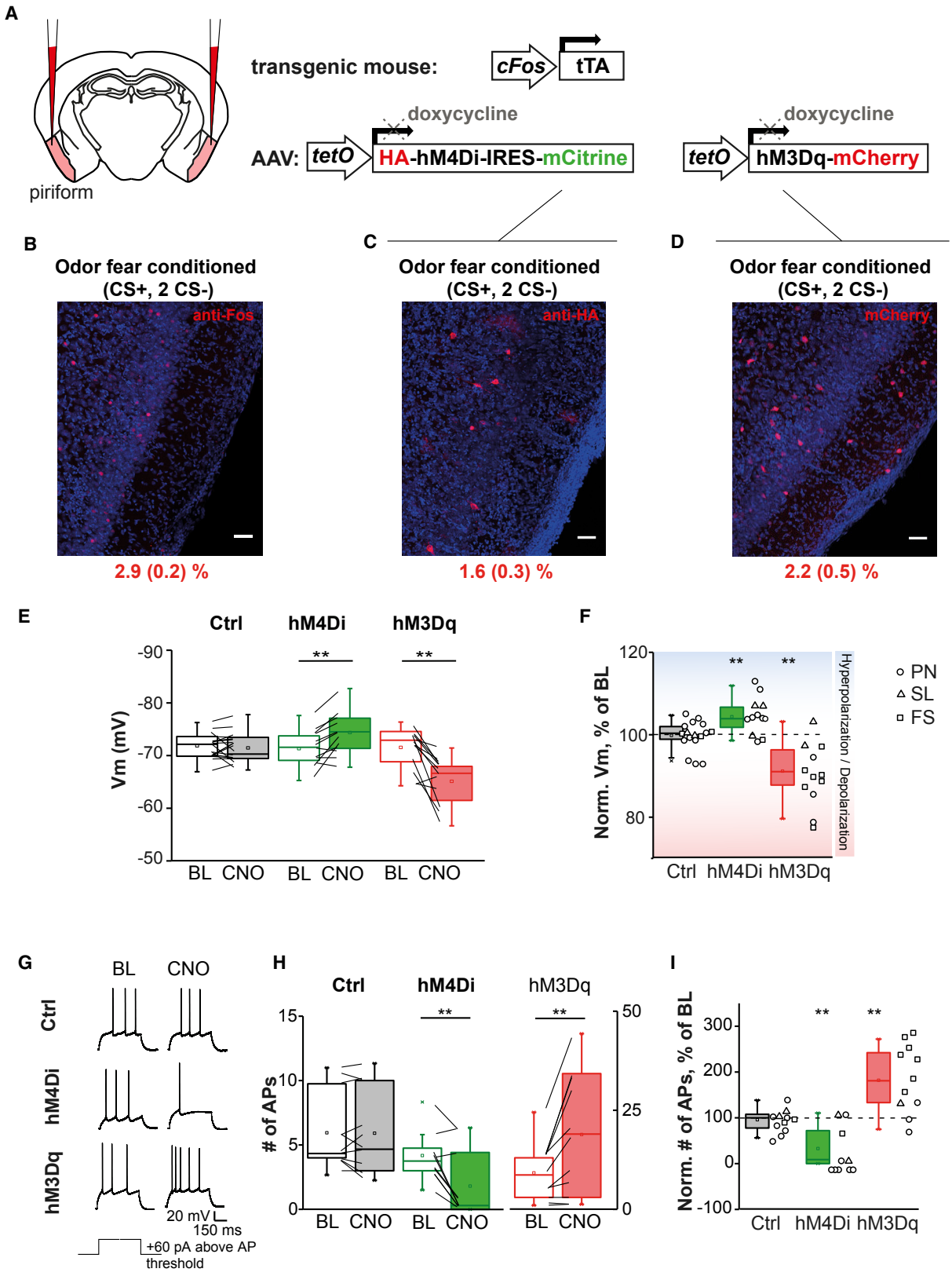

(legend on next page)

Fos-Expressing Piriform Neurons Can Be Tagged and Functionally Manipulated

If piriform neurons that were activated during olfactory learning encode an essential component of olfactory memories, then manipulating the activity of these neurons should impact memory recall.

Because the PCx is a large area, we used designer receptors exclusively activated by designer drugs (DREADDs) [23, 24] to manipulate its activity. DREADDs increase (hM3Dq:mCherry) or decrease (HA:hM4Di-IRES-mCitrine) the excitability of neurons upon activation by their ligand clozapine N-oxide (CNO). To selectively label piriform neurons that were activated during odor exposure, we used *cFos*-tTA transgenic mice [5] in which the activity-dependent *cFos* promoter drives expression of the tTA transcription factor, and we stereotaxically injected in the PCx adeno-associated viruses (AAVs) expressing DREADDs under the control of the tTA-responsive promoter tetO (Figure 2A). Temporal control of DREADD expression is provided by doxycycline, which interferes with the binding of tTA to tetO and thus suppresses transgene expression [27]. Mice maintained in their home cage on a doxycycline-containing diet showed low basal DREADD expression, detected by anti-hemagglutinin (HA) immunohistochemistry and native mCherry fluorescence (Figure S3C). To induce DREADD expression, mice were taken off doxycycline 5 days before odor presentation. Previous studies have shown that cFos-tTA-dependent expression of regulators of neural activity lasts for at least 5 days [4, 25, 28]. We therefore restricted our manipulations of neural activity to a 3-day time window after Fos tagging. Exposure to odor followed by foot shock resulted in the Fos tagging of sparse neural ensembles (median [interquartile range]: 1.6% [0.3%] of piriform neurons, n = 2 for hM4Di; 2.2% [0.5%] of piriform neurons, n = 3 for hM3Dq). Fos-tagged neurons were broadly dispersed throughout the anterior and posterior PCx (Figures 2C, 2D, and S3). The number and distribution of Fos-tagged cells were similar to endogenous Fos expression (2.9% [0.2%], n = 2; Figure 2B) [29, 30].

To test whether CNO-mediated activation of DREADDs in Fos-tagged piriform neurons alters their excitability, we performed whole-cell recordings in acute brain slices. DREADD-expressing neurons were identified based on mCitrine (HA:hM4Di-IRES-mCitrine) or mCherry (hM3Dq:mCherry) fluorescence. Fos-tagged neurons displayed diverse morphologies and electrophysiological properties and included both excitatory (pyramidal-like neurons, PNs; semilunar-like neurons, SLs) and inhibitory neurons (fast-spiking interneurons, FSs) (Figure S2). In the absence of CNO, the resting membrane potential of DREADD-negative neurons was indistinguishable from the resting potential of DREADD-expressing neurons (−72.14 [2.96] mV in DREADD-negative neurons, n = 17; −71.58 [4.50] mV in hM4Di-expressing neurons, n = 12; −72.56 [4.18] mV in hM3Dq-expressing neurons, n = 12; p = 0.819, Kruskal-Wallis ANOVA; Figure 2E). After bath application of CNO (5 μM), the resting membrane potential of DREADD-negative cells remained unchanged (WSRT, −72.27 [3.72] mV, n = 17, p = 0.818), whereas it changed in DREADD-expressing cells: hM4Di-expressing cells hyperpolarized and hM3Dq-expressing cells depolarized (WSRT, −74.51 [5.17] mV, n = 12, p = 0.011 and −66.95 [5.29] mV, n = 12, p = 0.005, respectively; Figure 2E). To determine the impact of CNO treatment on neuronal excitability, we delivered depolarizing current steps and compared the number of action potentials triggered by 60-pA step current above action potential threshold (see STAR Methods and Figure 2G). We found that in hM4Di-expressing cells, the number of evoked action potentials significantly decreased after CNO application, whereas in hM3Dq-expressing cells, it significantly increased (WSRT, 3.75 [1.59] versus 0.30 [3.48], n = 10, p = 0.010 and 8.67 [9.10] versus 19.0 [27.6] mV, n = 11, p = 0.006, respectively). In contrast, DREADD-negative cells did not exhibit a significant change in the number of evoked action potentials upon CNO application (WSRT, 4.33 [3.88] versus 4.67 [5.08], n = 11, p = 0.865; Figure 2H).

Performing one-sample WSRTs on the membrane potential and the number of action potentials after CNO application

Figure 2. Fos-Expressing Piriform Neurons Can Be Tagged and Functionally Manipulated

(A–D) Scheme of genetic strategy and histological characterization of Fos-tagged piriform ensembles.

(A) The "silencing" and "activating" TetTag system. AAVs (red) expressing DREADDs under the control of the tetO promoter were injected into the PCx of *cFos*-tTA transgenic mice (see also Figure S3). hM4Di or hM3Dq is expressed in active Fos-expressing piriform neurons upon doxycycline removal.

(B–D) Mice were fear conditioned to ethyl acetate 5 days after doxycycline removal. Training includes the presentation of two other odors that are not paired with foot shock (CS^-; eugenol and beta-citronellol). Mice were perfused 1 hr after the start of the experiment (B) or 3 days later (C and D).

(B) Endogenous Fos expression.

(C) Neurons expressing hM4Di were visualized using anti-HA immunohistochemistry.

(D) Neurons expressing hM3Dq were visualized with mCherry fluorescence. Neurotrace counterstain is in blue. Scale bars, 50 μm.

The numbers below the coronal sections indicate the median percentage (interquartile range) of tagged neurons quantified in 2 or 3 mice.

(E–I) Electrophysiological characterization of Fos-tagged piriform neurons. BL, pre-CNO baseline values; Ctrl, DREADD-negative cells.

(E) Resting membrane potential in mV, before and after CNO application. The resting membrane potential does not differ between DREADD-expressing and non-expressing cells. After CNO application, it does not change in DREADD-negative cells, whereas hM4Di-expressing cells hyperpolarize and hM3Dq-expressing cells depolarize.

(F) The normalized membrane potential in % to baseline in different cell types after CNO application. Pyramidal-like neurons (PNs) are marked as circles, semilunar-like cells (SLs) are marked as triangles, and fast-spiking interneurons (FSs) are shown as squares (see Figure S2).

(G–I) The excitability of DREADD-expressing cells is measured as the number of action potentials (APs) resulting from the third depolarizing current step, counting from the first step that elicits spiking (steps of 20 pA).

(G) Representative traces before and after CNO application.

(H) Number of APs before and after CNO application. After CNO application, the number of APs in DREADD-negative cells does not change, significantly decreases in hM4Di-expressing cells, and significantly increases in hM3Dq-expressing cells.

(I) Normalized number of APs in % to baseline in different cell types after CNO application. Cell types are marked as in (F).

Data are shown as individual data points and box and whiskers plots. Boxes are determined by the 1^{st} and 3^{rd} quartiles (median line), and the whiskers represent the 5^{th} and 95^{th} percentiles. **p < 0.01.

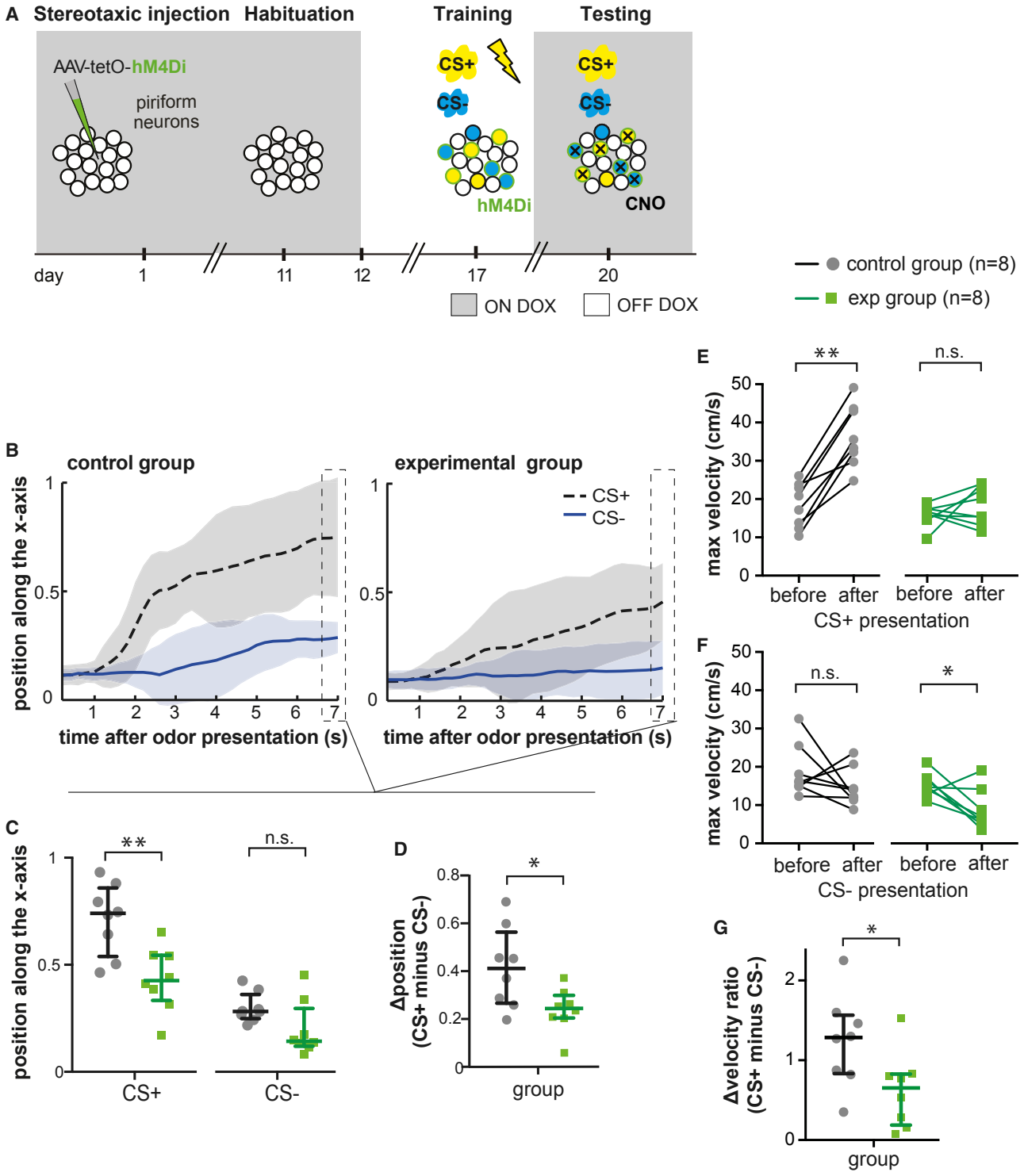

Figure 3. Silencing Fos-Tagged Piriform Ensembles Impairs Odor Fear Memory Recall

(A) Experimental design: *cFos*-tTA transgenic mice (experimental group, n = 8) or wild-type mice (control group, n = 8) are injected with AAV-tetO-hM4Di in both hemispheres of the PCx. Ten days later, mice are habituated to the training and testing boxes. Upon doxycycline (DOX) removal, mice are fear conditioned, and hM4Di expression (green circles) is induced in Fos-tagged neurons (filled in blue and yellow; see Figure S4). Mice are returned to a DOX-containing diet to avoid further expression of hM4Di. Three days later, all mice are intraperitoneally injected with CNO, which silences hM4Di-expressing neurons (black crosses), and memory retrieval is tested in the rectangular testing box (Figure 1B).

(legend continued on next page)

normalized to baseline values (in %) gave similar p values (Figures 2F and 2I). Although CNO effects were similar in different cell types (FS, PN, SL), sample sizes are insufficient to quantify or exclude cell-type-dependent variability.

Taken together, these experiments show that Fos tagging during olfactory fear conditioning marks a sparse and dispersed subpopulation of piriform neurons, and that CNO-mediated activation of hM4Di or hM3Dq expressed in Fos-tagged neurons selectively decreases or increases their excitability.

Silencing Fos-Tagged Piriform Ensembles Impairs Odor Fear Memory Recall

To test the effects of Fos-tagged ensemble manipulation on memory recall, we Fos tagged piriform neurons during olfactory fear conditioning and then chemogenetically silenced them during memory recall. *cFos*-tTA male mice ("experimental group," n = 8) were bilaterally injected in the PCx with the AAV-tetO-hM4Di vector. Wild-type male mice injected with the same virus served as a control ("control group," n = 8). Doxycycline was removed from the diet of mice prior to training, to permit the induction of hM4Di expression in Fos-expressing piriform neurons of mice of the experimental group. Mice were returned to doxycycline-containing diet immediately after odor fear conditioning, and memory recall of the odor-foot shock association was tested 3 days later in the rectangular testing box after intraperitoneal injection of CNO (Figure 3A). Mice from the control group received CNO injection to control for behavioral changes caused by potential off-target CNO effects [31]. For all mice, we verified viral gene expression by post hoc histological examination. Previous studies have suggested that the posterior PCx is important for associative memory encoding [10, 20, 32]. We therefore excluded from our analysis mice in which parts of the posterior PCx were spared from viral infection (Figures S3 and S4A).

As expected, control mice exhibited robust escape behavior upon CS^+ presentation (median position in the box at the end of CS^+ delivery: 0.74; increase in maximum velocity: 1.9-fold; Figures 3B, 3C, and 3E). In contrast, escape behavior was significantly reduced in mice in which Fos-tagged neurons were silenced. Their median position in the box at the end of stimulus delivery (0.42) and their increase in maximum velocity (1.1-fold) were significantly lower than in the control group (MWT, U = 7, p = 0.007 for both position and velocity; Figures 3B, 3C, and 3E). Subtracting the CS^- value from the CS^+ value for both position and maximum velocity ratio also led to significant differences between the control and experimental groups (MWT, U = 13, p = 0.0499 for position and U = 11, p = 0.0281 for maximum velocity ratio; Figures 3D and 3G). Differences in behavioral responses of *cFos*-tTA mice were specifically due to hM4Di activation, as escape behavior after CNO injection was unaffected in *cFos*-tTA mice injected with AAVs expressing the calcium indicator GCaMP (Figures 1C–1G).

Furthermore, all mice were similarly close to the odor port at the onset of CS^+ odor presentation (MWT, U = 28, p = 0.7209; Figure 3B), and had similar maximum velocities during the 7 s time period that preceded CS^+ presentation (MWT, U = 24, p = 0.4418; Figure 3E). These observations exclude any inherent differences between groups due to how the CS^+ was presented. Finally, we did not observe any differences in the overall mobility of mice throughout the entire testing session. The median speed of mice was not significantly different between the control and experimental groups (0.68 [0.28] cm/s and 0.46 [0.14] cm/s, respectively, MWT, U = 22, p = 0.3282), nor did mice show a bias for the left or right side of the testing box (time spent on the left side divided by time spent on the right side: 1.36 [0.72] and 1.51 [0.52] for the control and experimental groups, respectively, MWT, U = 27, p = 0.6454). Together, these data suggest that Fos-tagged piriform ensembles that were activated during olfactory fear conditioning are necessary for robust odor fear memory recall.

Even though *cFos*-tTA transgenic mice expressing hM4Di failed to robustly escape from the CS^+, it should be noted that they behaved differently after CS^+ and CS^- presentation. They were farther away from the odor port after CS^+ presentation than after CS^- presentation (WSRT, W = −36, p = 0.0078; Figure 3C), and their maximum velocity ratio was significantly higher (after/before odor presentation, WSRT, W = −36, p = 0.0078; Figures 3E–3G). This could indicate a partial memory of the learned association, possibly due to incomplete silencing of functionally relevant neurons in the PCx, or the existence of parallel neural pathways that partially compensate for the loss of PCx functions.

Memory Impairments Are Specific to the Piriform Ensemble Fos Tagged during Learning

Silencing the PCx in only one brain hemisphere did not abolish the learned escape behavior to the conditioned odor (Figure S5). Furthermore, memory impairments were not related to the bilateral or unilateral infection of brain regions adjacent to the PCx due to spillover of the virus (parts of the cortical and basolateral amygdala, and insular cortex; Figure S5). Therefore, memory impairments are most likely specific to the PCx.

We next wanted to determine whether the memory deficits were specific to the neurons that were Fos tagged during learning. Odors activate unique yet overlapping ensembles of piriform neurons [33–35]. Therefore, silencing neurons that respond to

(B–G) Olfactory memory retrieval after CNO injection, assessed by the position of the mice in the testing box and their maximum velocity upon odor exposure. Memory retrieval was significantly impaired in *cFos*-tTA mice in which piriform neurons that were active during learning were chemogenetically silenced during memory recall (experimental group). See Figure S5 for unilaterally infected mice.

(B) Averaged position of mice in the testing box as a function of time after CS^+ (black dashed line) and CS^- (blue line) presentation.

(C–G) Control group: color coded black; experimental group: color coded green.

(C) Position in the testing box 7 s after CS^+ or CS^- presentation.

(D) Position 7 s after CS^- presentation subtracted from the position 7 s after CS^+ presentation.

(E) Maximum velocity during a 7 s time window before and after CS^+ presentation.

(F) Maximum velocity during a 7 s time window before and after CS^- presentation.

(G) Maximum velocity ratio after/before CS^- subtracted from the maximum velocity ratio after/before CS^+ presentation.

Dots represent individual mice, and averaged data are shown as median and interquartile range. *p < 0.05, **p < 0.01; n.s., not significant.

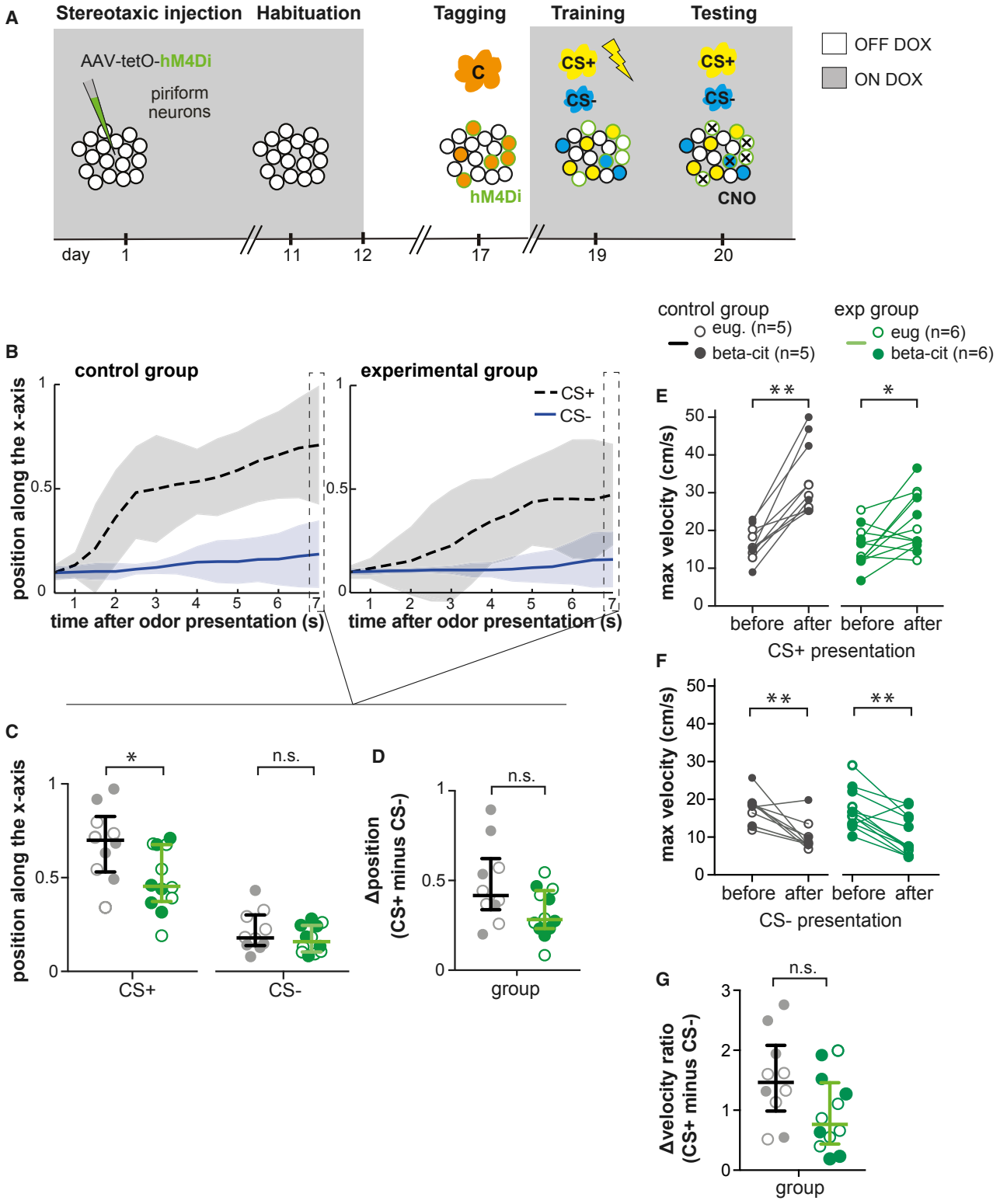

Figure 4. Memory Impairments Are Specific to the Piriform Ensemble that Is Fos Tagged during Learning

(A) Experimental design: dissociating Fos tagging and fear conditioning. Upon DOX removal, mice are presented with an odor in a neutral environment (C: eugenol [eug.] or beta-citronellol [beta-cit.]). hM4Di expression (green circles) is induced in Fos-tagged neurons (filled in orange; also see Figures S3 and S4). Two days later, mice are fear conditioned to ethyl acetate (CS$^-$: limonene and beta-cit. when Fos tagged with eug., and limonene and eug. when Fos tagged with beta-cit.). One day later, memory retrieval is tested in the presence of CNO, which silences hM4Di-expressing neurons (black crosses).

(legend continued on next page)

one odor could partially interfere with the retrieval of information associated with other odors. To test this, we modified the behavioral protocol to separate Fos tagging from fear conditioning. *cFos*-tTA transgenic and wild-type control mice were injected with AAV-tetO-hM4Di and expression of hM4Di in piriform neurons was induced while mice were exposed to eugenol or beta-citronellol in a neutral environment, without subsequent foot shock. Mice were returned to a doxycycline-containing diet and fear conditioned 2 days later to ethyl acetate (CS^+). Behavioral testing of memory recall was performed 1 day later, after intraperitoneal injection of CNO (Figure 4A). Fos tagging resulted in the labeling of sparse neural ensembles, similar in numbers to those tagged during olfactory fear conditioning (1.1% [0.3%] of piriform neurons, n = 3; Figures S3D and S4B). We found that the learned escape behavior of *cFos*-tTA mice (experimental group, n = 12) was similar but somewhat attenuated compared to controls (n = 10). Both groups exhibited an escape behavior after CS^+ presentation, indicated by the significant increase in the maximum velocity (WSRT, W = 55, p = 0.0020 and W = 54, p = 0.0342 for control and experimental groups, respectively; no difference in the CS^+ minus CS^- velocity ratio between groups, MWT, U = 33, p = 0.0804; Figures 4E–4G). The difference in the position of the mice after CS^+ and CS^- presentation was also similar between groups (MWT, U = 37, p = 0.1402; Figure 4D). However, we observed that silencing neutral odor representations somewhat dampened the behavioral response to the CS^+, as behavioral responses were less robust compared to controls when quantifying the position of the mice in the box after CS^+ presentation (MWT, U = 22, p = 0.0112; Figures 4B and 4C). The attenuated behavioral responses that we observe most likely reflect the partial degradation of odor information as a result of the silencing of piriform neurons responsive to both the CS^+ and the neutral odor.

Silencing Fos-Tagged Piriform Ensembles Does Not Alter Odor Detection and Discrimination

Chemogenetic silencing of piriform ensembles Fos tagged during olfactory fear conditioning could disrupt odor detection and discrimination rather than selectively affecting odor fear memory recall. To test this possibility, we monitored the sniffing behavior of mice during an olfactory habituation assay (Figure 5A), a well-established test for odor detection and discrimination [36, 37]. Fos tagging of piriform neurons during olfactory fear conditioning was performed as described in Figure 3A. Three days later, changes in sniffing behavior in response to odor exposure were tested in a plethysmograph while Fos-tagged neurons were silenced with CNO (see Figure S4C and STAR Methods). We observed that mice of both the experimental (n = 8) and control (n = 6) groups increased their sniff frequency upon the first presentation of pinene, a novel and neutral odor (1.6-fold increase relative to pre-odor baseline frequency; Figures 5B and 5D). Repeated exposure to the same odor (pinene or CS^-) resulted in a decrease in sniff frequency, reflecting habituation after 4 consecutive exposures (WSRT for the neutral odor, W = −21, p = 0.0312 for the control and W = −36, p = 0.0078 for the experimental group; Figure 5D). Subsequent presentation of the CS^+ increased the sniff frequency (1.4-fold increase relative to the fourth CS^- presentation; WSRT, W = 21, p = 0.0312 for the control and W = 34, p = 0.0156 for the experimental group; Figure 5E). Such changes in odor-sampling behavior have been shown to report the detection and discrimination of different odor stimuli [36–38].

Furthermore, the baseline sniff frequency, the difference in sniff frequency between the first and fourth exposures of the same odor, and the difference in sniff frequency between the CS^- after habituation and the CS^+ were similar between control and experimental groups (MWT; U = 12.5, p = 0.1512 for baseline; U = 22, p = 0.8228 for pin4 − pin1; and U = 24, p > 0.9999 for $CS^+ - CS^-4$; Figure 5C).

These data suggest that basic behaviors characteristic of odor sampling, detection, and discrimination were unaffected by the silencing of piriform ensembles that were Fos tagged during olfactory fear conditioning.

Reactivation of Fos-Tagged Piriform Ensembles Mimics Odor-Evoked Fear Memory Recall

If piriform neural ensembles that were activated during olfactory fear conditioning encode an essential component of odor fear memories, then reactivation of these neurons may be sufficient to trigger memory recall.

To test this, we infected the PCx of *cFos*-tTA female mice with the activating DREADD AAV-tetO-hM3Dq (Figure S4D). We first trained mice to associate ethyl acetate with foot shock, without CS^- presentation. We then intraperitoneally injected CNO to reactivate hM3Dq-expressing piriform neurons that were Fos tagged during learning (Figure 6A). Chemogenetics does not provide precise temporal control of neuronal activity, and CNO binding leads to a prolonged modulation of neuronal activation [23]. We therefore tested artificial memory retrieval in the open-field box (see Figures 1H–1K for memory retrieval tested with prolonged odor exposure).

11.7% (1.7%) of hM3Dq-expressing cells were reactivated upon CNO injection. As a point of comparison, 1.8% (1.4%) of neurons were reactivated during olfactory memory retrieval (Figure S6). CNO-mediated reactivation, similar to CS^+ exposure, caused a significant decrease in exploratory behavior of fear-conditioned mice (n = 7), compared to baseline exploratory behavior measured 1 day earlier (WSRT, W = −26, p = 0.0312; Figure 6B). In contrast, reactivation of piriform neurons that were Fos tagged during ethyl acetate exposure without foot

(B–G) Olfactory memory retrieval after CNO injection, assessed by the position of mice in the testing box and their maximum velocity. Memory retrieval was moderately attenuated in *cFos*-tTA mice expressing hM4Di in neurons that were Fos tagged during presentation of a neutral odor (experimental group, n = 12), compared to wild-type mice (control group, n = 10). Color code is as in Figure 3.
(B) Averaged position of mice as a function of time after CS^+ and CS^- presentation.
(C) Position of mice in the testing box 7 s after CS^+ or CS^- presentation.
(D) Position 7 s after CS^- presentation subtracted from the position 7 s after CS^+ presentation.
(E) Maximum velocity during the 7 s before and after CS^+ presentation.
(F) Maximum velocity during the 7 s before and after CS^- presentation.
(G) Maximum velocity ratio after/before CS^- subtracted from the maximum velocity ratio after/before CS^+ presentation.
Dots represent individual mice, and averaged data are shown as median and interquartile range. *p < 0.05, **p < 0.01; n.s., not significant.

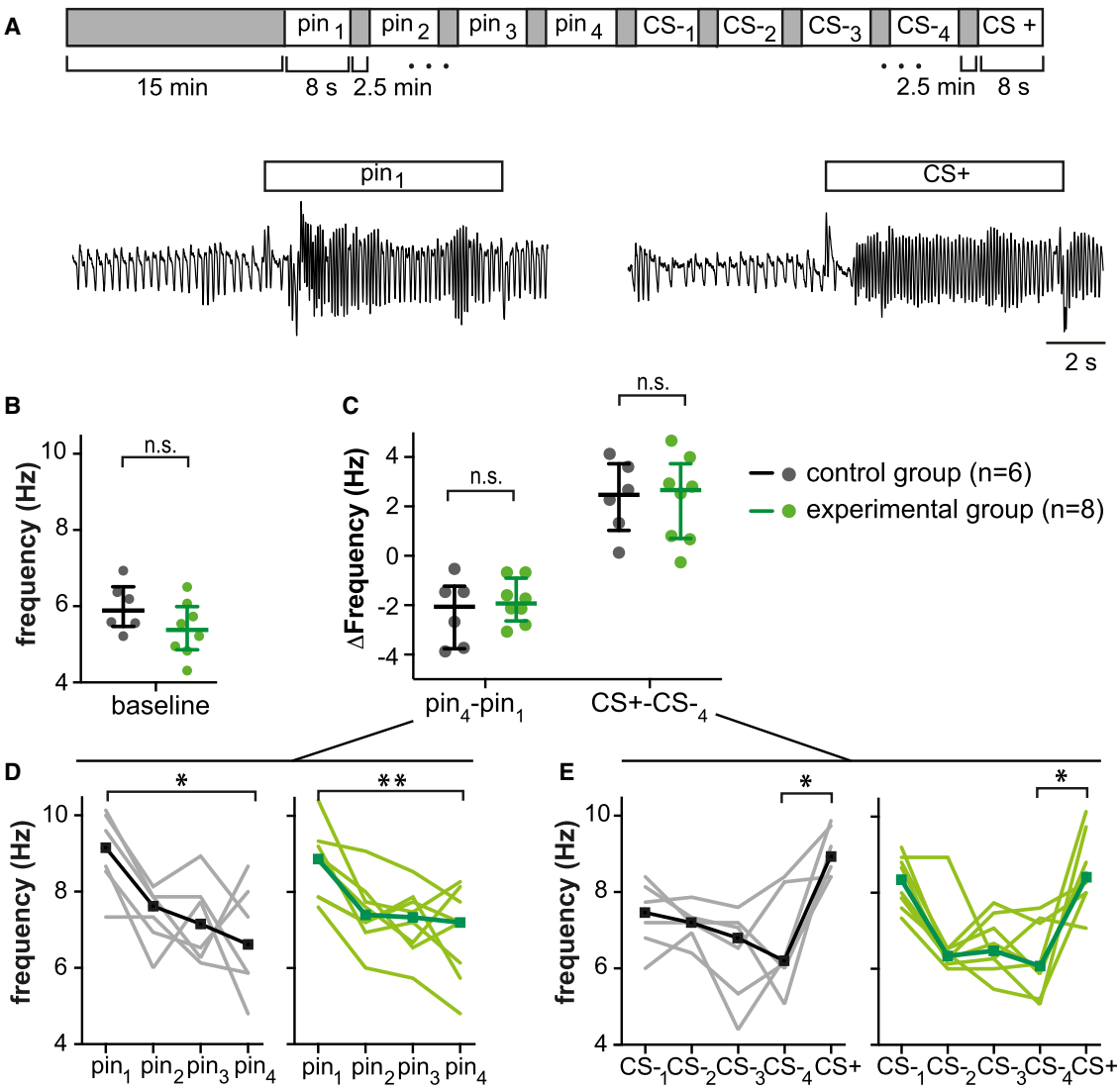

Figure 5. Silencing Fos-Tagged Piriform Ensembles Does Not Interfere with Odor Detection and Discrimination

(A) Top: experimental design: Fos tagging during olfactory fear conditioning is performed as described in Figure 3 (see also Figure S4). Three days after fear conditioning, sniffing behavior is quantified in a plethysmograph. Mice are intraperitoneally injected with CNO and habituated to the plethysmograph for 15 min, and each odor is then presented for 8 s with a 2.5 min inter-trial interval. Pin, pinene; CS^-, beta-citronellol; CS^+, ethyl acetate. Bottom: representative sniff recordings from one mouse when exposed to pinene (1st presentation) or the CS^+.

(B and C) Dots represent individual mice, and averaged data are shown as median and interquartile range.

(D and E) Each thin line represents data of individual mice; the squares and thick lines represent averaged data (median).

(B) Baseline sniff frequency, corresponding to the averaged sniff frequency 8 s before odor onset.

(C–E) For both the control (n = 6) and experimental groups (n = 8), repeated exposure to the same odor resulted in a decrease in the sniff frequency (habituation), whereas presentation of a different odor resulted in an increase in the sniff frequency.

(C) The changes in sniff frequency after presentation of the same or a different odor are similar between the experimental and control groups. The sniff frequency during the fourth presentation of pinene is subtracted from its first presentation (pin4 − pin1), or the sniff frequency during the fourth presentation of the CS^- is subtracted from the sniff frequency during the CS^+ presentation ($CS^+ - CS^-4$).

(D) Sniff frequency for the first to fourth presentation of pinene: control (left) and experimental group (right).

(E) Sniff frequency for the first to fourth presentation of the CS^-, and subsequent presentation of the CS^+: control (left) and experimental group (right).

*p < 0.05, **p < 0.01; n.s., not significant.

shock (n = 7) did not affect exploratory behavior (WSRT, W = −10, p = 0.4688; Figure 6B). Exploratory behavior after CNO injection normalized to baseline was significantly different between the control and experimental groups (MWT, U = 8, p = 0.0379; Figure 6C). These data suggest that chemogenetic reactivation of piriform neurons that were active during odor-foot shock exposure is sufficient to trigger fear memory recall.

We next asked whether artificial memory recall depends on the specificity of the Fos-tagged neural ensemble: is piriform reactivation sufficient to trigger fear memory recall, as long as it

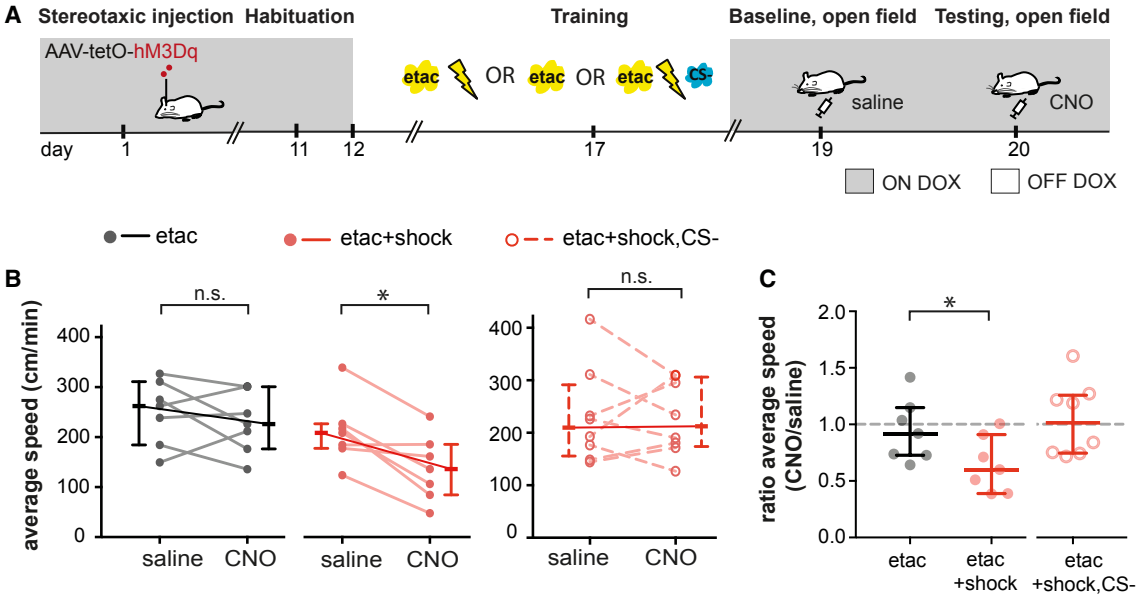

Figure 6. Reactivation of Fos-Tagged Piriform Ensembles Mimics Odor-Evoked Fear Memory Recall

(A) Experimental design: artificial odor fear memory recall tested in an open-field assay (see Figure 1). *cFos*-tTA transgenic mice are injected with AAV-tetO-hM3Dq into the PCx to induce hM3Dq expression in Fos-expressing neurons during training (see also Figures S3 and S4). Mice are trained to associate ethyl acetate with foot shock (CS^+), and mice exposed to ethyl acetate without foot shock serve as controls. An additional group is trained to associate ethyl acetate with foot shock, and training includes the presentation of two CS^- (eugenol and beta-citronellol). Two days later, baseline exploratory activity in an open field is measured during 22 min, 5 min after intraperitoneal injection of saline (baseline). The next day (testing), CNO is intraperitoneally injected to reactivate Fos-tagged, hM3Dq-expressing piriform neurons (see Figure S6), and the activity of mice in the open field is measured again.

(B) Average speed in cm/min: distance traveled during the entire testing session divided by the duration of the session. CNO injection leads to a decrease in exploratory behavior in mice previously fear conditioned to ethyl acetate in the absence of CS^- (n = 7). Previous exposure to ethyl acetate without foot shock does not alter exploratory behavior upon reactivation of Fos-tagged piriform ensembles (n = 7).

Reactivation of piriform ensembles Fos tagged during olfactory fear conditioning including reinforced (CS^+) and non-reinforced (CS^-) odor stimuli does not affect exploratory behavior (n = 8).

(C) Average speed ratio testing/baseline.

Dots represent individual mice, and averaged data are presented as median and interquartile range. *$p < 0.05$; n.s., not significant.

includes the CS^+-tagged ensemble? For this purpose, we generated a synthetic Fos-tagged ensemble, by alternating exposure to the CS^+ odor paired with foot shock with exposure to CS^- neutral odors. We found that artificial reactivation of a synthetic Fos-tagged ensemble did not result in changes in exploratory behavior indicative of memory recall (WSRT, n = 8, W = −4, p = 0.8438; Figure 6B). These data suggest that during artificial reactivation, the PCx cannot extract meaningful information from the synthetic representation generated by the sequential presentation of CS^+ and CS^- odors.

DISCUSSION

The PCx has long been thought to provide the substrate for storing associative olfactory memories, yet the cellular substrates for olfactory learning and memory remain unknown. Using a *cFos*-dependent, intersectional genetic approach to visualize and manipulate piriform neurons activated during olfactory fear conditioning, we found that chemogenetic silencing of Fos-tagged ensembles robustly diminished a learned odor escape behavior without altering basic odor detection and discrimination. Furthermore, chemogenetic reactivation of Fos-tagged piriform ensembles resulted in reduced exploratory behavior in an open-field assay, an effect that was similarly observed when exposing mice to the conditioned odor stimulus. Together, our experiments identify piriform neurons expressing Fos during learning as an essential neural circuit component for triggering odor fear memory recall.

Localization of the Odor Fear Memory Trace

The behavioral consequences of manipulating Fos-tagged piriform neurons suggest the formation of functional connections between piriform neurons and other association areas. Candidate target areas for the processing of odor-fear associations include the basolateral amygdala and the medial prefrontal cortex [39, 40]; however, the relevant neural circuit components remain to be identified. We propose that odor fear memories are encoded in distributed ensembles of neurons throughout the brain, with different regions contributing to different components of the overall memory. The PCx could store information about odor objects, whereas associated emotions of past olfactory experiences could be stored in the amygdala (see [2, 41] for a similar model relative to contextual and auditory fear conditioning). Several studies have shown that PCx cells can encode information that carries behavioral significance [20, 32, 42]. Future studies investigating learning-induced changes in cellular and

network properties of Fos-tagged neurons will establish whether their silencing modifies the perception of the CS^+, and thus the reactivation of the memory linked to the CS^+, or whether a memory trace of the odor-foot shock association is also formed within the Fos-tagged piriform ensembles.

Technical Limitations of Fos Tagging for Studying Odor Fear Memories

In this study, we used two different fear-conditioning paradigms and two different retrieval contexts. It has previously been shown that the absence or presence of odorants not paired with foot shock (CS^-) leads to a more or less generalized fear of odors similar to the reinforced conditioned stimulus (CS^+) and to differential changes in the responses of piriform neurons [17]. Thus, the PCx might be differentially involved in the retrieval of olfactory memories, depending on the presence or absence of the CS^-. In rats, the PCx is not necessary 3 days after fear conditioning to a CS^+ odor without the CS^-, yet becomes indispensable when memory is tested 1 month after learning [20]. In our hands, Fos-tagged piriform ensembles are essential for odor fear memory retrieval 3 days after learning, when the CS^+-shock presentation is coupled to the presentation of the CS^-.

A general limitation of the *cFos*-tTA system is that the tagging of neurons is transient. The duration of the expression of tTA-dependent proteins is determined by the time course of induction and the stability of cFos-tTA-dependent transcripts and proteins. Previous studies have shown that cFos-tTA-dependent expression of regulators of neural activity becomes undetectable by 30 days [4, 25]. Therefore, the temporal involvement of the PCx in memory retrieval cannot be addressed with Fos tagging.

Another constraint of the Fos-tagging system is its slow temporal dynamics. As a consequence, when training included the presentation of the CS^-, neurons responding to the CS^- were tagged in addition to neurons responding to the CS^+. We showed that the additional CS^- "background" neurons had no significant impact on the outcome of the silencing experiment, as chemogenetic silencing of neurons activated during presentation of a CS^- only moderately attenuated odor fear memory recall.

Interestingly, the number of Fos-expressing and Fos-tagged piriform neurons we observe is significantly lower than the number of odor-responsive neurons detected in electrophysiological recordings in awake mice [33, 43, 44]. However, in these experiments, a large fraction of cells exhibited low firing rates. Therefore, the Fos-tagged population could represent a subpopulation of neurons that is strongly activated by odor [45]. Fos tagging could also mark plastic changes supporting memory formation [46, 47]. Indeed, *cFos* mRNA levels decrease after injection of an antagonist of the NMDA receptor, a key player in the induction of synaptic plasticity [48], and long-term memory and synaptic plasticity are impaired when cFos production is perturbed in the central nervous system [49].

Artificial Reactivation of an Olfactory Memory Trace

Reactivation of neurons by CNO-mediated activation of DREADD receptors does not recapitulate the temporal characteristics of piriform odor responses and their modulation by active sampling [33, 43]. Despite this, reactivation of piriform ensembles Fos tagged during odor-foot shock pairing was sufficient to elicit a behavioral response. How piriform neural circuits and downstream target regions process such artificial activity patterns remains to be determined. One possibility is that despite the temporal limitations of memory trace reactivation, piriform network mechanisms can retrieve the perception of the reinforced conditioned stimulus. Consistent with this model, recent studies have shown that spatial patterns of odor-evoked activity, in the absence of precise temporal information, are sufficient to decode odor identity [33, 34, 43]. Alternatively, it is possible that reactivation generates a state of fear, but without evoking the perception of the odor. Finally, reactivating a synthetic ensemble of neurons activated during exposure to both CS^+ and CS^- did not elicit a measurable behavioral response. This observation suggests that behaviorally relevant information cannot be extracted from a neural ensemble representing conflicting (aversive versus neutral) information, and further supports the specificity of the Fos-tagged ensemble. This result is consistent with the finding that the reactivation of an artificial contextual memory in the hippocampus competes with the retrieval of a learned context-shock association [50].

Memory Traces in the Hippocampus and PCx

The hippocampus has been studied extensively for its role in spatial and contextual memory [51]. Recently, Fos tagging of hippocampal neurons during contextual fear conditioning has provided important insight into the cellular and neural circuit mechanisms of learning and memory [4, 22, 50, 52–54]. However, whether principles of memory formation and storage in hippocampus-related neural networks apply to other cortical structures remains largely unknown. Interestingly, the PCx and hippocampus share a similar circuit organization and both have been modeled as auto-associative networks [10]. In both regions, learning marks sparse and distributed ensembles of neurons that appear to lack topographic organization. Furthermore, hippocampal neurons tagged during contextual fear conditioning and piriform neurons tagged during olfactory fear conditioning were both necessary and sufficient for memory retrieval [4, 6]. Our findings thus reveal striking similarities between memory traces of contextual fear in the hippocampus and olfactory memory traces in the PCx.

STAR★METHODS

Detailed methods are provided in the online version of this paper and include the following:

- KEY RESOURCES TABLE
- CONTACT FOR REAGENT AND RESOURCE SHARING
- EXPERIMENTAL MODEL AND SUBJECT DETAILS
- METHOD DETAILS
  - Constructs and viruses
  - Stereotaxic injection
  - Immunohistochemistry
  - Electrophysiology
  - Behavioral apparatus
  - Behavioral procedures
  - Drugs
- QUANTIFICATION AND STATISTICAL ANALYSIS
  - Cell counting
  - Electrophysiology

SUPPLEMENTAL INFORMATION

Supplemental Information includes six figures and can be found with this article online at https://doi.org/10.1016/j.cub.2018.12.003.

ACKNOWLEDGMENTS

We thank Mark Mayford for sharing the *cFos*-tTA transgenic mouse line, and Brian Roth and Susumu Tonegawa for sharing plasmids. We thank Yves Dupraz and Gérard Parésys for their work on the behavioral apparatuses, Agatha Anet for help with behavioral experiments, Tristan Piolot for help with image acquisition, Philippe Mailly for help with cell quantification, and Marion Ruinart de Brimont for help with cloning. We thank Karim Benchenane and Sophie Bagur for sharing their plethysmograph. We thank Rainer Friedrich, Anne Didier, Kevin Franks, Boris Gourévitch, Andreas Schaefer, and Claire Zhang for careful reading and critical comments on the manuscript. This work was supported by the Amorçage de Jeunes Équipes program (AJE201106) of the Fondation pour la Recherche Médicale (to A.F.) and a postdoctoral fellowship by LabEx MemoLife (to C.M.-B.).

AUTHOR CONTRIBUTIONS

Conceptualization, C.M.-B. and A.F.; Methodology, Investigation, and Analysis, C.M.-B. and Y.D. (electrophysiology); Writing – Original Draft, C.M.-B. and A.F., with contributions from Y.D. and L.V.; Supervision and Funding Acquisition, C.M.-B., L.V., and A.F.

DECLARATION OF INTERESTS

The authors declare no competing interests.

Received: June 2, 2018
Revised: October 19, 2018
Accepted: December 4, 2018
Published: January 3, 2019

REFERENCES

1. Mouly, A.-M., and Sullivan, R. (2010). Memory and plasticity in the olfactory system: from infancy to adulthood. In The Neurobiology of Olfaction Frontiers in Neuroscience, A. Menini, ed. (CRC Press/Taylor & Francis).
2. Mayford, M., and Reijmers, L. (2015). Exploring memory representations with activity-based genetics. Cold Spring Harb. Perspect. Biol. *8*, a021832.
3. Tonegawa, S., Pignatelli, M., Roy, D.S., and Ryan, T.J. (2015). Memory engram storage and retrieval. Curr. Opin. Neurobiol. *35*, 101–109.
4. Liu, X., Ramirez, S., Pang, P.T., Puryear, C.B., Govindarajan, A., Deisseroth, K., and Tonegawa, S. (2012). Optogenetic stimulation of a hippocampal engram activates fear memory recall. Nature *484*, 381–385.
5. Reijmers, L.G., Perkins, B.L., Matsuo, N., and Mayford, M. (2007). Localization of a stable neural correlate of associative memory. Science *317*, 1230–1233.
6. Tanaka, K.Z., Pevzner, A., Hamidi, A.B., Nakazawa, Y., Graham, J., and Wiltgen, B.J. (2014). Cortical representations are reinstated by the hippocampus during memory retrieval. Neuron *84*, 347–354.
7. Apicella, A., Yuan, Q., Scanziani, M., and Isaacson, J.S. (2010). Pyramidal cells in piriform cortex receive convergent input from distinct olfactory bulb glomeruli. J. Neurosci. *30*, 14255–14260.
8. Davison, I.G., and Ehlers, M.D. (2011). Neural circuit mechanisms for pattern detection and feature combination in olfactory cortex. Neuron *70*, 82–94.
9. Wilson, D.A., and Sullivan, R.M. (2011). Cortical processing of odor objects. Neuron *72*, 506–519.
10. Haberly, L.B. (2001). Parallel-distributed processing in olfactory cortex: new insights from morphological and physiological analysis of neuronal circuitry. Chem. Senses *26*, 551–576.
11. Johnson, D.M., Illig, K.R., Behan, M., and Haberly, L.B. (2000). New features of connectivity in piriform cortex visualized by intracellular injection of pyramidal cells suggest that "primary" olfactory cortex functions like "association" cortex in other sensory systems. J. Neurosci. *20*, 6974–6982.
12. Sadrian, B., and Wilson, D.A. (2015). Optogenetic stimulation of lateral amygdala input to posterior piriform cortex modulates single-unit and ensemble odor processing. Front. Neural Circuits *9*, 81.
13. Johenning, F.W., Beed, P.S., Trimbuch, T., Bendels, M.H.K., Winterer, J., and Schmitz, D. (2009). Dendritic compartment and neuronal output mode determine pathway-specific long-term potentiation in the piriform cortex. J. Neurosci. *29*, 13649–13661.
14. Kanter, E.D., and Haberly, L.B. (1990). NMDA-dependent induction of long-term potentiation in afferent and association fiber systems of piriform cortex in vitro. Brain Res. *525*, 175–179.
15. Quinlan, E.M., Lebel, D., Brosh, I., and Barkai, E. (2004). A molecular mechanism for stabilization of learning-induced synaptic modifications. Neuron *41*, 185–192.
16. Chapuis, J., and Wilson, D.A. (2011). Bidirectional plasticity of cortical pattern recognition and behavioral sensory acuity. Nat. Neurosci. *15*, 155–161.
17. Chen, C.-F.F., Barnes, D.C., and Wilson, D.A. (2011). Generalized vs. stimulus-specific learned fear differentially modifies stimulus encoding in primary sensory cortex of awake rats. J. Neurophysiol. *106*, 3136–3144.
18. Sevelinges, Y., Gervais, R., Messaoudi, B., Granjon, L., and Mouly, A.-M. (2004). Olfactory fear conditioning induces field potential potentiation in rat olfactory cortex and amygdala. Learn. Mem. *11*, 761–769.
19. Shakhawat, A.M.D., Gheidi, A., MacIntyre, I.T., Walsh, M.L., Harley, C.W., and Yuan, Q. (2015). Arc-expressing neuronal ensembles supporting pattern separation require adrenergic activity in anterior piriform cortex: an exploration of neural constraints on learning. J. Neurosci. *35*, 14070–14075.
20. Sacco, T., and Sacchetti, B. (2010). Role of secondary sensory cortices in emotional memory storage and retrieval in rats. Science *329*, 649–656.
21. Choi, G.B., Stettler, D.D., Kallman, B.R., Bhaskar, S.T., Fleischmann, A., and Axel, R. (2011). Driving opposing behaviors with ensembles of piriform neurons. Cell *146*, 1004–1015.
22. Garner, A.R., Rowland, D.C., Hwang, S.Y., Baumgaertel, K., Roth, B.L., Kentros, C., and Mayford, M. (2012). Generation of a synthetic memory trace. Science *335*, 1513–1516.
23. Alexander, G.M., Rogan, S.C., Abbas, A.I., Armbruster, B.N., Pei, Y., Allen, J.A., Nonneman, R.J., Hartmann, J., Moy, S.S., Nicolelis, M.A., et al. (2009). Remote control of neuronal activity in transgenic mice expressing evolved G protein-coupled receptors. Neuron *63*, 27–39.
24. Ferguson, S.M., Eskenazi, D., Ishikawa, M., Wanat, M.J., Phillips, P.E.M., Dong, Y., Roth, B.L., and Neumaier, J.F. (2011). Transient neuronal inhibition reveals opposing roles of indirect and direct pathways in sensitization. Nat. Neurosci. *14*, 22–24.
25. Zhang, Z., Ferretti, V., Güntan, İ., Moro, A., Steinberg, E.A., Ye, Z., Zecharia, A.Y., Yu, X., Vyssotski, A.L., Brickley, S.G., et al. (2015). Neuronal ensembles sufficient for recovery sleep and the sedative actions of $\alpha 2$ adrenergic agonists. Nat. Neurosci. *18*, 553–561.
26. Adolphs, R. (2013). The biology of fear. Curr. Biol. *23*, R79–R93.
27. Gossen, M., Freundlieb, S., Bender, G., Müller, G., Hillen, W., and Bujard, H. (1995). Transcriptional activation by tetracyclines in mammalian cells. Science *268*, 1766–1769.
28. Cowansage, K.K., Shuman, T., Dillingham, B.C., Chang, A., Golshani, P., and Mayford, M. (2014). Direct reactivation of a coherent neocortical memory of context. Neuron *84*, 432–441.

29. Datiche, F., Roullet, F., and Cattarelli, M. (2001). Expression of Fos in the piriform cortex after acquisition of olfactory learning: an immunohistochemical study in the rat. Brain Res. Bull. *55*, 95–99.
30. Illig, K.R., and Haberly, L.B. (2003). Odor-evoked activity is spatially distributed in piriform cortex. J. Comp. Neurol. *457*, 361–373.
31. Gomez, J.L., Bonaventura, J., Lesniak, W., Mathews, W.B., Sysa-Shah, P., Rodriguez, L.A., Ellis, R.J., Richie, C.T., Harvey, B.K., Dannals, R.F., et al. (2017). Chemogenetics revealed: DREADD occupancy and activation via converted clozapine. Science *357*, 503–507.
32. Calu, D.J., Roesch, M.R., Stalnaker, T.A., and Schoenbaum, G. (2007). Associative encoding in posterior piriform cortex during odor discrimination and reversal learning. Cereb. Cortex *17*, 1342–1349.
33. Bolding, K.A., and Franks, K.M. (2017). Complementary codes for odor identity and intensity in olfactory cortex. eLife *6*, e22630.
34. Roland, B., Deneux, T., Franks, K.M., Bathellier, B., and Fleischmann, A. (2017). Odor identity coding by distributed ensembles of neurons in the mouse olfactory cortex. eLife *6*, e26337.
35. Stettler, D.D., and Axel, R. (2009). Representations of odor in the piriform cortex. Neuron *63*, 854–864.
36. Coronas-Samano, G., Ivanova, A.V., and Verhagen, J.V. (2016). The habituation/cross-habituation test revisited: guidance from sniffing and video tracking. Neural Plast. *2016*, 9131284.
37. Wesson, D.W., Donahou, T.N., Johnson, M.O., and Wachowiak, M. (2008). Sniffing behavior of mice during performance in odor-guided tasks. Chem. Senses *33*, 581–596.
38. Verhagen, J.V., Wesson, D.W., Netoff, T.I., White, J.A., and Wachowiak, M. (2007). Sniffing controls an adaptive filter of sensory input to the olfactory bulb. Nat. Neurosci. *10*, 631–639.
39. Dejean, C., Courtin, J., Karalis, N., Chaudun, F., Wurtz, H., Bienvenu, T.C.M., and Herry, C. (2016). Prefrontal neuronal assemblies temporally control fear behaviour. Nature *535*, 420–424.
40. Gore, F., Schwartz, E.C., Brangers, B.C., Aladi, S., Stujenske, J.M., Likhtik, E., Russo, M.J., Gordon, J.A., Salzman, C.D., and Axel, R. (2015). Neural representations of unconditioned stimuli in basolateral amygdala mediate innate and learned responses. Cell *162*, 134–145.
41. Tonegawa, S., Liu, X., Ramirez, S., and Redondo, R. (2015). Memory engram cells have come of age. Neuron *87*, 918–931.
42. Mandairon, N., Kermen, F., Charpentier, C., Sacquet, J., Linster, C., and Didier, A. (2014). Context-driven activation of odor representations in the absence of olfactory stimuli in the olfactory bulb and piriform cortex. Front. Behav. Neurosci. *8*, 138.
43. Miura, K., Mainen, Z.F., and Uchida, N. (2012). Odor representations in olfactory cortex: distributed rate coding and decorrelated population activity. Neuron *74*, 1087–1098.
44. Zhan, C., and Luo, M. (2010). Diverse patterns of odor representation by neurons in the anterior piriform cortex of awake mice. J. Neurosci. *30*, 16662–16672.
45. Schoenenberger, P., Gerosa, D., and Oertner, T.G. (2009). Temporal control of immediate early gene induction by light. PLoS ONE *4*, e8185.
46. Cole, A.J., Saffen, D.W., Baraban, J.M., and Worley, P.F. (1989). Rapid increase of an immediate early gene messenger RNA in hippocampal neurons by synaptic NMDA receptor activation. Nature *340*, 474–476.
47. Minatohara, K., Akiyoshi, M., and Okuno, H. (2016). Role of immediate-early genes in synaptic plasticity and neuronal ensembles underlying the memory trace. Front. Mol. Neurosci. *8*, 78.
48. Tayler, K.K., Lowry, E., Tanaka, K., Levy, B., Reijmers, L., Mayford, M., and Wiltgen, B.J. (2011). Characterization of NMDAR-independent learning in the hippocampus. Front. Behav. Neurosci. *5*, 28.
49. Fleischmann, A., Hvalby, O., Jensen, V., Strekalova, T., Zacher, C., Layer, L.E., Kvello, A., Reschke, M., Spanagel, R., Sprengel, R., et al. (2003). Impaired long-term memory and NR2A-type NMDA receptor-dependent synaptic plasticity in mice lacking c-Fos in the CNS. J. Neurosci. *23*, 9116–9122.
50. Ramirez, S., Liu, X., Lin, P.-A., Suh, J., Pignatelli, M., Redondo, R.L., Ryan, T.J., and Tonegawa, S. (2013). Creating a false memory in the hippocampus. Science *341*, 387–391.
51. Basu, J., and Siegelbaum, S.A. (2015). The corticohippocampal circuit, synaptic plasticity, and memory. Cold Spring Harb. Perspect. Biol. *7*, a021733.
52. Cai, D.J., Aharoni, D., Shuman, T., Shobe, J., Biane, J., Song, W., Wei, B., Veshkini, M., La-Vu, M., Lou, J., et al. (2016). A shared neural ensemble links distinct contextual memories encoded close in time. Nature *534*, 115–118.
53. Roy, D.S., Kitamura, T., Okuyama, T., Ogawa, S.K., Sun, C., Obata, Y., Yoshiki, A., and Tonegawa, S. (2017). Distinct neural circuits for the formation and retrieval of episodic memories. Cell *170*, 1000–1012.e19.
54. Ryan, T.J., Roy, D.S., Pignatelli, M., Arons, A., and Tonegawa, S. (2015). Memory. Engram cells retain memory under retrograde amnesia. Science *348*, 1007–1013.
55. Meziane, H., Ouagazzal, A.-M., Aubert, L., Wietrzych, M., and Krezel, W. (2007). Estrous cycle effects on behavior of C57BL/6J and BALB/cByJ female mice: implications for phenotyping strategies. Genes Brain Behav. *6*, 192–200.
56. Padilla, S.L., Qiu, J., Nestor, C.C., Zhang, C., Smith, A.W., Whiddon, B.B., Rønnekleiv, O.K., Kelly, M.J., and Palmiter, R.D. (2017). AgRP to Kiss1 neuron signaling links nutritional state and fertility. Proc. Natl. Acad. Sci. USA *114*, 2413–2418.
57. Srinivasan, S., and Stevens, C.F. (2018). The distributed circuit within the piriform cortex makes odor discrimination robust. J. Comp. Neurol. *526*, 2725–2743.
58. Suzuki, N., and Bekkers, J.M. (2006). Neural coding by two classes of principal cells in the mouse piriform cortex. J. Neurosci. *26*, 11938–11947.

STAR★METHODS

KEY RESOURCES TABLE

REAGENT or RESOURCE	SOURCE	IDENTIFIER
Antibodies		
rabbit anti-HA	Cell Signaling Technology	Cat# 3724; RRID: AB_1549585
rabbit anti-GFP	Invitrogen	Cat# A-6455; RRID: AB_221570
goat anti-cFos	Santa Cruz Biotechnology	Cat# sc-52-G; RRID: AB_2629503
Alexa Fluor 488-conjugated secondary antibodies	Invitrogen	Cat# A-21206 & A-11055; RRID: AB_2535792 & AB_2534102
Alexa Fluor 568-conjugated secondary antibodies	Invitrogen	Cat# A10042; RRID: AB_2534017
NeuroTrace 640/660	Invitrogen	N21483
Bacterial and Virus Strains		
AAV-tetO-hM3Dq:mCherry	Penn Vector Core	this paper
AAV-tetO-HA:hM4Di-IRES-mCitrine	Penn Vector Core	this paper
Chemicals, Peptides, and Recombinant Proteins		
Clozapine-N-oxide	SIGMA	C0832
Dimethyl sulfoxide	SIGMA	D2438
Experimental Models: Organisms/Strains		
cfos-tTA mice		N/A
Oligonucleotides		
DNA primers	Eurofins	N/A
Recombinant DNA		
pAAV-pTRE-tight-hM3Dq-mCherry	Addgene	RRID: Addgene_66795
Software and Algorithms		
MATLAB	The MathWorks	https://fr.mathworks.com/products/matlab.html?s_tid=hp_products_matlab
Prism 7	Graphpad	https://www.graphpad.com/scientific-software/prism/
Software for mouse tracking	This paper	https://git.io/fxVeE
ImageJ plugin for quantification	This paper	available upon request
Other		
Doxycycline 1g/kg	SSNIFF	A112D71003

CONTACT FOR REAGENT AND RESOURCE SHARING

Further information and requests for resources and reagents should be directed to and will be fulfilled by the Lead Contact, Alexander Fleischmann (alexander_fleischmann@brown.edu).

EXPERIMENTAL MODEL AND SUBJECT DETAILS

Mice were housed at 24°C with a 12-hour light/12-hour dark cycle with standard food and water provided *ad libitum*. Mice were group-housed with littermates until the beginning of surgery and then single-housed in ventilated cages throughout the duration of the experiment. *cFos*-tTA mice [5] were originally generated on a mixed C57BL/6 x DBA/2 genetic background and backcrossed for at least 6 generations into a pure C57BL/6N genetic background (Charles River). Wild-type control animals (n = 46) were siblings that did not carry the *cFos*-tTA transgene. The age of mice at the time of behavioral testing ranged from 10 to 15 weeks. Male mice (n = 48) were used for the hM4Di-mediated neural silencing, and littermate females (n = 40) for the hM3Dq-mediated neural activation experiments. No differences in open field performance depending on the phase of the estrous cycle were found in female mice [55], and CNO injection does not disrupt the estrous cycle [56]. Mice were fed a diet containing 1g/kg doxycycline (SSNIFF) for a minimum of 4 days before surgery. Experiments were carried out according to European and French national institutional animal care guidelines (protocol APAFIS#2016012909576100).

METHOD DETAILS

Constructs and viruses

The hSynapsin promoter of pAAV-hSyn-HA-hM4Di-IRES-mCitrine (kindly provided by Dr. B. Roth, University of North Carolina at Chapel Hill) was excised using the restriction enzyme XbaI (New England Biolabs) and replaced by the Tetracycline Response Element of a pAAV-TRE-EYFP (excised with Xba1 et Nhe1, plasmid kindly provided by Dr. S. Tonegawa, MIT, Cambridge). The pAAV-pTRE-tight-hM3Dq-mCherry [25] was purchased from Addgene (#66795). Adeno-associated viruses (AAVs) were generated at Penn Vector Core, University of Pennsylvania (serotype 8, 10^{13} genome copies/mL, 1:2 dilution with sterile PBS on the day of injection).

Stereotaxic injection

Mice were anaesthetized with ketamine/xylazine (100 mg/kg/10 mg/kg, Sigma-Aldrich) and AAV vectors were injected stereotaxically into the piriform cortex (PCx, coordinates relative to bregma: anterior-posterior, −0.6 mm; dorsal-ventral, −4.05 mm; lateral, 4.05 mm and −4.05 mm). Using a micromanipulator and injection assembly kit (Narishige; WPI), a pulled glass micropipette (Dutscher, 075054) was slowly lowered into the brain and left for 30 s in place before infusion of the virus at an injection rate of 0.2-0.3 μL per min. 0.8-1 μL of virus was sufficient to infect a large area of PCx. The micropipette was left in place for an additional 3-4 min and then slowly withdrawn to minimize diffusion along the injector tract.

Immunohistochemistry

Mice were deeply anesthetized with pentobarbital and perfused transcardially with phosphate-buffered saline (PBS) followed by 4% paraformaldehyde. Brains were post-fixed 4 hr in 4% paraformaldehyde, and 100-200 μm coronal sections were cut with a vibrating blade microtome (Microm Microtech). Sections were permeabilized in 0.1% Triton X-100/PBS (PBST) for 1 h, then blocked in 2% heat-inactivated horse serum (HIHS)-PBST for 1 hr. Sections were incubated in 2% HIHS-PBST containing polyclonal primary antibodies (rabbit anti-HA, 1:200, Cell Signaling; rabbit anti-GFP, 1:1000, Invitrogen; goat anti-cFos, 1:500, Santa Cruz) with gentle agitation at 4°C overnight. Next, sections were rinsed 3 times in PBST for 20 min, blocked in 2% HIHS-PBST for 1 h, and incubated in NeuroTrace 640/660 (Invitrogen) and species-appropriate Alexa Fluor 488 (green) and Alexa Fluor 568 (red)-conjugated secondary antibodies (1:1000, Invitrogen) at 4°C overnight. Sections were washed 2 times in PBST and 1 time in PBS, mounted on slides and coverslipped with Vectashield mounting medium (Vectorlabs). Images were acquired as Z stacks (70 to 140 μm in total thickness, step size 7 μm) with a Leica SP5 confocal microscope or as single plane sections with a Zeiss Axio Zoom microscope and processed in Fiji.

Electrophysiology

Parasagittal or coronal slices (300 μm thick) of PCx were prepared from 6-8 week-old *cFos*-tTA mice injected with AAV-tetO-HA:hM4Di-IRES-mCitrine or AAV-tetO-hM3Dq:mCherry. Three days after olfactory fear conditioning, animals were anaesthetized with ketamine and xylazine (100 mg/kg/10 mg/kg, Sigma-Aldrich), perfused with ice-cold ACSF (125 mM NaCl, 2.5 mM KCl, 25 mM glucose 25mM $NaHCO_3$, 1.25 mM NaH_2PO_4, 2 mM $CaCl_2$, 1 mM $MgCl_2$, 1 mM pyruvic acid, bubbled with 95% O_2 and 5% CO_2 and adjusted to 295 ± 5 mOsm osmolarity), and decapitated. The brain was cooled with ice-cold ACSF solution and then sliced using a 7000SM2 vibrating microtome (Campden Instruments, UK). Slices were incubated in the same solution at 34°C for 1 hr and then continuously perfused with ACSF solution (2 mL/min) at 34°C in the recording chamber. DREADD expression was detected with two-photon excitation (830nm, ChameleonMRU-X1, Coherent, UK) under a Scientifica TriM Scope II microscope (LaVision, Germany), with a 60x water-immersion objective. Whole-cell recording pipettes with 5-7 MΩ resistance were filled with the following solution (in mM): 122 Kgluconate, 13 KCl, 10 HEPES, 10 phosphocreatine, 4 Mg-ATP, 0.3 Na-GTP, 0.3 EGTA (adjusted to pH 7.35 with KOH). The recording solution also contained the morphological tracer Alexa Fluor 594 (5 μM, red channel) for non-expressing and hM4Di-positive cells or the Ca^{2+}-sensitive dye Fura-2 (300 μM, replacing EGTA in the recording solution, green channel) for hM3Dq-positive cells, to enable identification of the patched cell and to visualize its morphology. The excitability of cells was measured in current-clamp mode by 500 ms steps of current injections from −300 to +500 pA with steps of 20 pA. We compared the number of action potentials triggered by equivalent depolarization at each step 60 pA above the action potential threshold before and after CNO (5 μM) application. The series resistance was usually < 20 MΩ, and data were discarded if it changed by more than 20% during the recording. Signals were amplified using EPC10-2 amplifiers (HEKA Elektronik, Lambrecht, Germany). Voltage-clamp recordings were filtered at 5 kHz and sampled at 10 kHz, and current-clamp recordings were filtered at 10 kHz and sampled at 20 kHz, with the Patchmaster v2x32 program (HEKA Elektronik).

Behavioral apparatus

A training box was used to train mice to escape from an odor. The box was rectangular (L 57 cm, W 17 cm, H 64 cm), with a grid floor made of 72 stainless-steel rods (diameter = 6 mm, space between rods = 2 mm) and walls made of gray Altuglas Visio. Current was delivered by an aversive stimulator (MedAssociates, 115V, 60 Hz). A custom-made switcher allowed an electric foot shock (0.6 mA, 0.6 ms) to be applied independently to either half of the box. A testing box was used to test memory retrieval. Its dimensions were the same as the training box. Materials for the walls (black expanded PVC) and floor (white Altuglas) were different from the training box to create a different context. Odor ports were located at each extremity of the training and testing boxes.

The open field box consisted of a white Plexiglas (6 mm thickness) container (50 cm x 50 cm x 38 cm height).

Sniffing behavior was monitored in freely moving mice using a plethysmograph (Emka Technologies). Electrical signals were amplified using RHD 2132 amplifier boards (Intan Technologies) and band-pass filtered (1-30 Hz).

Odors were delivered using an 8 channels olfactometer (Automate Scientific). The olfactometer output was split into two channels downstream of the odor bottles, and controlled by independent valve controllers for left/right presentation. A continuous clean air stream and the output from the olfactometer valves converged into a custom-made manifold. To avoid pressure changes when presenting the odors, a valve connected to a bottle of mineral oil (Sigma-Aldrich) was opened when the valves connected to the odor bottles were closed. The following odors (Sigma-Aldrich), at a concentration of 1% (vol/vol) in mineral oil were used: ethyl acetate, beta-citronellol, eugenol, limonene, and pinene.

Behavioral procedures

AAVs were stereotaxically injected in both hemispheres of PCx of *cFos*-tTA transgenic mice and littermate wild-type controls. Mice were given 10 days to recover, before being habituated on day 11 to the training and testing/open field/plethysmograph boxes (40 and 10 min each). 24 hr after habituation, doxycycline was removed and replaced by a regular diet. Five days later, mice were fear conditioned to ethyl acetate or exposed to an odor (odor "C") in a neutral environment. Immediately after fear conditioning or odor presentation, mice were put back on a diet containing doxycycline. During fear conditioning, mice were freely moving in the conditioning box. Ethyl acetate (the CS+) was presented when the mouse was located at one end of the box, and the corresponding half-side of the box' floor was electrified for 0.6 s (0.6 mA). The foot shock was delivered 4 s after CS+ presentation, and the CS+ lasted for an additional 2 s. Mice learned to escape to the opposite side when the CS+ was presented. The CS+ was presented 4 times, 2 times on each side of the box. When fear conditioning included presentation of two non-reinforced conditioned stimuli (CS-), the choice between CS+ and CS- as well as the side of presentation was pseudo-randomized. Training always started with one presentation of each CS- followed by the CS+. The two CS- odors were presented during 7 s, 3 times each, with a total presentation of 3 on the right side and 3 on the left side. The mean time interval between two odor presentations was 3 min.

In the rectangular testing box, the CS+ was presented 4 times (2 times on each side), and each CS- was presented once on each side, for 7 s each (mean time interval between two odors: 3 min). As for the training session, the order and side of odor presentations was pseudo-randomized: testing always started with one presentation of each CS-, followed by one CS+ presentation. In the open field, the olfactometer outputs were placed above the open field box. Mice were placed in the middle of the box at the start of each session.

Drugs

Clozapine-N-oxide (C0832, Sigma-Aldrich) was first dissolved in dimethylsulfoxide (DMSO, D2438, Sigma, final concentration of 1% vol/vol), then further diluted in 0.9% sterile saline solution to a final concentration of 0.2 mg/mL. Aliquots were stored for up to two months at -20°C and equilibrated to room temperature before injection. The solution was administered intraperitoneally (3 mg/kg). After injection, mice were left undisturbed for 25 min (Figures 3 and 4) or 5 min (Figures 5 and 6) in their home cage before the start of the experiment.

QUANTIFICATION AND STATISTICAL ANALYSIS

Cell counting

Z stacks (7 μm step) were acquired with a Leica SP5 confocal microscope with a 20X objective and a resolution of 512x512 or 1024x1024 pixels (1 pixel: 0.72μm). First, the PCx was delineated on a maximum projection of each stack using a custom-written ImageJ macro. For each mouse, 2 to 4 sections (median volume 9.3e-2 (9.4e-3) mm^3) were analyzed, from one or both hemispheres, at Y = -0.8 and Y = -1.6mm relative to bregma.

HA-stained neurons (hM4Di) were counted by hand. hM3Dq-mCherry and Fos-positive neurons were counted using a custom-written ImageJ plugin. After pre-processing the image (Subtract Background, Remove Outliers and Median Filter), the z stack is thresholded using the RenyiEntropy algorithm. On each slice of the stack, objects with an area smaller than 35μm^2 are removed using the Analyze Particle command in ImageJ. A mask of each slice from the stack is created containing the filled outline of the measured particles. The number of cells is the number of 3D objects detected in the stack. Automated cell detection can be prone to errors; thus, the detection efficiency was checked on a few pictures by two people blind to the experimental conditions. An estimate E_{TOT} of the total number of neurons (counterstained with NeuroTrace) per cubic millimeter (7.1e4 mm^{-3}) was obtained by counting neurons in representative volumes containing the three layers of PCx. Numbers are consistent with those obtained by [57]. The total number of neurons in each stack was calculated by multiplying E_{TOT} by the volume of the stack.

Electrophysiology

Electrophysiological data were analyzed with custom-made software in Python 3.0 and averaged in MS Excel (Microsoft, USA). Cell types were classified based on their excitability, input resistance, the resting membrane potential, as described in [58] and morphology obtained from 2-photon images

Behavioral data

Behavioral sessions were video recorded and analyzed using custom-written MATLAB programs (https://git.io/fxVeE). Parameters extracted from multiple CS+ (CS-) presentations were averaged for each mouse, when testing occurred in the rectangular testing box (Figures 1, 3, and 4).

Statistics

Statistical analysis was performed with Prism (GraphPad). Non-parametric tests were used: Mann-Whitney test (MWT) for between group comparison, and Wilcoxon matched-pairs signed rank test (WSRT) for within group comparison. Values are represented as median (interquartile range) unless otherwise stated. The n represents number of mice, or number of recorded neurons for the electrophysiology experiment.

DATA AND SOFTWARE AVAILABILITY

Data are available upon request.